Numerical analysis of collisionless particle motion in an observed supercritical shock front

M. Gedalin

Department of Physics, Ben-Gurion University, Beer-Sheva, Israel

J. A. Newbury and C. T. Russell

Institute of Geophysics and Planetary Physics, University of California, Los Angeles

1. Introduction

The basic model (and the only well-developed model) of quasi-perpendicular collisionless shocks is the stationary one-dimensional shock model, which assumes that the electric and magnetic fields in the shock front depend on the single coordinate x along the shock normal and do not depend on time. Rankine-Hugoniot relations connecting upstream and downstream plasma parameters imply stationarity and one dimensionality, at least at spatial scales substantially larger than the upstream convective ion gyroradius V_u/Ω_u (V_u being the upstream plasma velocity along the shock normal, and $\Omega_u = eB_u/m_i$ being the upstream ion gyrofrequency) and at temporal scales substantially larger than the upstream ion gyroperiod $2\pi/\Omega_u$. Real shocks always contain nonstationary and three-dimensional features in the form of waves. However, it is widely believed that the basic features of the shock are due to the ion and electron interaction with the quasi-stationary fields, even in the narrow ramp. This strong assumption leads to a number of unambiguous consequences. First, this means that the pressure balance

$$nm_iV_x^2 + p_{i,xx} + p_{e,xx} + \mathbf{B}^2/2\mu_0 = \text{const} \tag{1}$$

should be satisfied throughout the shock profile. Here n is the electron (and ion because of quasi-neutrality) density, V_x is the plasma velocity along the shock normal, $p_{e,xx}$ and $p_{i,xx}$ are the corresponding components of the electron and ion pressure, and $\mathbf{B}$ is the local magnetic field. This pressure balance has been checked [*Scudder et al.*, 1986a] by comparing the total pressures well upstream and well downstream of an observed high Mach number shock, and it has been found to be satisfied within 20% error. However, it was never checked throughout the shock profile, partly because the particle measurement resolution (3 s for ISEE and 4.5 s for Active Magnetospheric Particle Tracer Explorers (AMPTE)) is significantly lower than the typical scale $\lesssim 1$ s of the small-scale structure [*Newbury et al.*, 1998].

Second, the stationary one-dimensional shock model implies that the ion dynamics (reflection and gyration) are determined by the stationary electric and magnetic field [*Leroy et al.*, 1982; *Sckopke et al.*, 1983; *Burgess et al.*, 1989; *Sckopke et al.*, 1990; *Gedalin*, 1996a], which means that ion heating [see, e.g., *Gedalin*, 1997a, and references therein] and foot formation [*Woods*, 1971; *Sckopke et al.*, 1983] are primarily due to the magnetic compression and cross-shock potential and only weakly depend on the wavy features in the shock front. The derived expressions [*Woods*, 1971; *Sckopke et al.*, 1983; *Gosling and Thomsen*, 1985] for the foot length crucially depend on the above assumptions.

Third, it is widely believed that electron dynamics are collisionless and are also determined by the cross-shock electric field and magnetic field of the stationary and one-dimensional shock structure [*Feldman et al.*, 1982; *Goodrich and Scudder*, 1984; *Feldman*, 1985; *Scudder et al.*, 1986b, c; *Thomsen et al.*, 1987; *Schwartz et al.*, 1988; *Balikhin et al.*, 1993; *Gedalin et al.*, 1995; *Scudder*, 1995; *Hull et al.*, 1998]. If this is the case, the increase of the electron energy (and therefore the electron heating) while crossing the shock is completely determined by the de Hoffman-Teller cross-shock potential. Independent of the mechanism of the electron heating (adiabatic in wide shocks or nonadiabatic in very narrow shocks), the high-energy tail of the downstream electron distribution is determined by the collisionless Liouville mapping of the upstream distribution. These collisionless dynamics result in the formation of a gap in the downstream distribution and are unable to explain the distribution smoothing and gap filling. Some nonstationary and/or non-one-dimensional features should be responsible for the downstream distribution formation, although typical frequencies of these features may be much higher than the typical ion times, and spatial scales may be much smaller than the electron inertial length c/ω_{pe} [*Veltri et al.*, 1990, 1992 ; *Veltri and Zimbardo*, 1993a, b].

Observations show [*Newbury et al.*, 1998] that at least some of high Mach number shocks are quasi-stationary; that is, they vary slowly at the ion gyroperiod. They often possess [*Gedalin et al.*, 1998; *Newbury et al.*, 1998] small-scale structure with the typical scale, which is estimated as $\sim 0.1 - 0.2(c/\omega_{pi})$ (sometimes this scale is as small as c/ω_{pe} [*Newbury and Russell*, 1996]). It is more difficult to estimate deviations from one dimensionality from the same two-spacecraft measurements. In several cases, when the spatial separation between the spacecraft along the shock front is of the order of ion inertial length c/ω_{pi} [*Gedalin et al.*, 1998; *Newbury et al.*, 1998], it was concluded that the typical scale of variation along the shock front is greater than V_u/Ω_u. In these cases the wave amplitude is low (waves are the features which vary at a timescale significantly faster than the timescale of shock front variation) and are expected to not be able to intervene into energetic ion processes at the ramp.

It has been shown [*Zilbersher et al.*, 1998] that the stationary one-dimensional model works well for low Mach number shocks. This was shown by tracing ions across the observed shock profile and checking the pressure balance throughout the shock front. In the present paper we analyze the collisionless ion and electron behavior in an observed high Mach number shock front. The main objective is to determine whether the ion dynamics in the structured magnetic field of the shock may be consistent with the assumptions of quasi-stationarity and one dimensionality and to understand the role of the small-scale features. The applied step-by-step method is as follows. The first stage is preparation: choose an observed high Mach number shock (high-resolution vector magnetic field); check (quasi-)stationarity and one dimensionality (if possible); filter out apparently nonstationary features (hopefully not much) and assume the rest strictly stationary and one-dimensional; and add electric field from observations if possible (3 components needed) or from a suitable model. The second stage is numerical analysis: choose upstream particle distributions (ions and electrons) according to the measurements of plasma parameters; and numerically analyze the collisionless dynamics of the particles in the prepared field structure. The third stage includes further analysis: analyze ion transmission (deceleration and residual downstream gyration) and reflection; analyze downstream density, bulk velocity, temperature, and pressure of ions; and analyze adiabaticity and nonadiabaticity in the electron behavior and gap in the downstream distribution. The analysis should allow us to conclude whether ion and electron heating can be due to only collisionless dynamics in stationary and one-dimensional profile and what the role is of the small-scale structure.

The paper is organized as follows. We describe the observed shock profile and our model assumptions in section 2. Numerical tracing of ions in this shock is described in section 3, and electron dynamics are considered in section 4. We discuss the results and implications for the model in section 5.

2. Observed Shock

We have chosen the shock observed by ISEE 1 on January 6, 1978, 0701:30 UT. This shock is quasi-perpendicular, $\theta_{Bn} = 58^\circ$, and supercritical, $M_A = 3.3$. The upstream plasma is rather cold: $\beta_e = 0.19$ and $\beta_i = 0.05$. The magnetic field (total and three components), rotated to the normal shock coordinates (where x is along the shock normal and y is the noncoplanarity direction), is shown in Figure 1. Time is measured in seconds and the measurement resolution is four

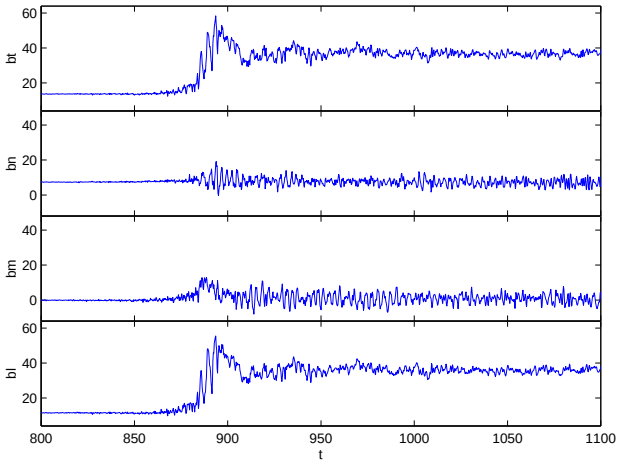

Figure 1. Magnetic field of the shock observed by ISEE 1 on January 6, 1978, 0701:30 UT, rotated to the normal shock coordinates, where x is along the shock normal and y is the noncoplanarity direction. Time is measured in seconds starting at 0647 UT. Resolution is four vectors per second.

magnetic field vectors per second.

The spatial separation along the shock normal $\approx$ 116 km between ISEE 1 and 2 was substantially greater than an ion inertial length, $c/\omega_{pi} \approx 84$ km, allowing one to see the evolution of the shock profile, if any. Time separation between the ramp observations by ISEE 1 and 2 was $\approx 15\,s$ (three upstream gyroperiods), which is also suitable for a reliable analysis of the slow evolution of the shock front. The profiles measured by the two spacecraft are similar, as can be seen from Figure 2, which suggests that the shock profile is quasi-stationary. Additional argument in favor of this conclusion follows from the consideration of the wavelet transform of the two profiles shown in Figure 3. The applied g_1 transform [*Gedalin et al.*, 1998] is not sensitive to quasiperiodic (wavy) features and picks up only large-amplitude steep structures. The wavelet spectral density is shown by shading (the gray scale limits are the same for both profiles as is seen from the gray scale bars), while time (position) and scale (duration) are shown on the x and y axes in seconds. It is clearly seen that at scales less than 5 s the two wavelet transforms show the same pattern: the overall ramp including all small-scale features lasts for sim 3.5-4

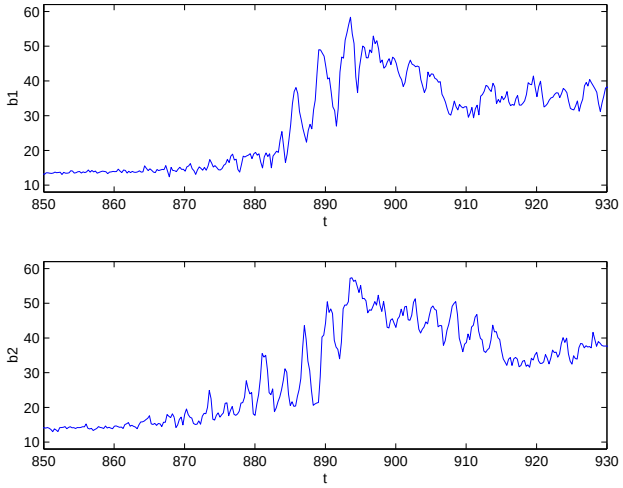

Figure 2. Comparison of ISEE 1 and 2 profiles of the total magnetic field. ISEE 2 profile shifted by $\sim$ 15 s. Spacecraft separation along the normal is $> c/\omega_{pi}$. Time separation is three ion gyroperiods. Similarity of the two profiles indicates quasi-stationarity.

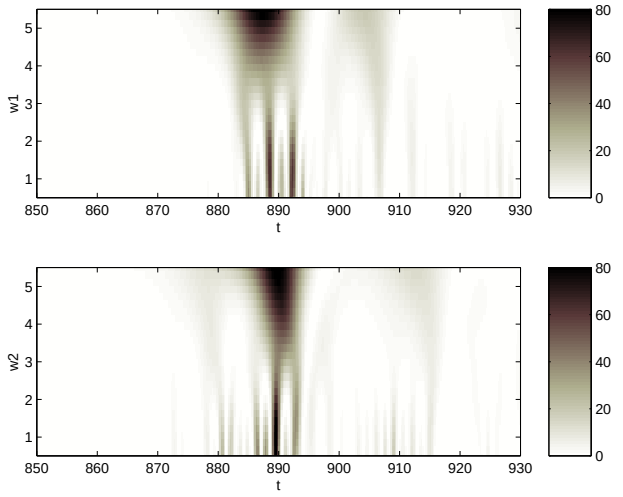

Figure 3. Comparison of wavelet transforms (g_1 transform) of ISEE 1 and 2 total magnetic field. ISEE 2 profile shifted by $\sim$ 15 s. The transform is sensitive to large-amplitude steep features and insensitive to quasiperiodic wave trains. Bright features correspond to the steep small-scale structure. Clear similarity (mutual disposition and scale) implies quasi-stationarity of the subramp structure.

s and is positioned at the same point for ISEE 1 and 2. At finer scales the pattern consists of three distinct features, the mutual disposition of which changes slightly from ISEE 1 profile to ISEE 2 profile by $\sim$ 1-2 s during 15 s of time separation and indicates slow temporal variation of the profile. Since the typical time of the ramp crossing by a transmitted ion or an electron is $\sim (c/\omega_{pi})/V_u \sim (1/2\pi M_A)T_u$ (where $T_u = 2\pi/\Omega_u$ is the upstream gyroperiod), this variation is expected to not significantly affect the process of ramp crossing for these particles. Reflected ions might be affected, in principle, since the typical time of their return to the ramp is $\sim T_u$. Yet, apparently the temporal changes are slow enough for the shock to be considered stationary, at least in the lowest-order approximation.

One dimensionality is more difficult to establish. In fact, the above consideration is unable to distinguish between spatial variations along the shock front (because of which different magnetic field profiles may be measured by the two spacecraft as functions of time) and true temporal variations. In what follows we assume that the shock is stationary and one dimensional. The degree of inconsistency, if any, of the collisionless particle motion with the observed shock profile will show us to what extent the temporal variations and three-dimensional shape of the shock can be ignored. We note that reduction of dimensionality to any value less than 3 imposes severe constraints on particle motion, affecting conclusions

about particle acceleration [*Jokipii et al.*, 1993; *Jones et al.*, 1998], which (acceleration) is, however, beyond the scope of the present paper.

The next step is to remove the small-scale (high frequency in the spacecraft frame) variations of the magnetic field which we can hardly expect to be quasi-stationary. This is done using discrete wavelet transform and removing several of the finest scales. The method proved to be efficient [*Gedalin et al.*, 1998] in filtering the profile while retaining the essential substructure present in the ramp. The results of such filtering are shown in Figure 4. It is this magnetic field which is used

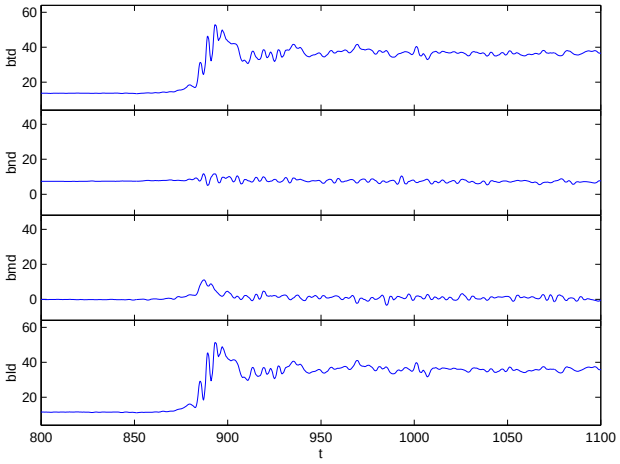

Figure 4. Magnetic field of the shock observed on January 6, 1978, 0701:30 UT, rotated to the normal shock coordinates (x is along the shock normal and y is along the noncoplanarity direction) and filtered using wavelet transform (Daubechies 10 wavelet) and removing the two finest levels. The remaining structure is assumed to be stationary and one dimensional.

in the subsequent numerical analysis of the ion and electron motions in the shock front.

The magnetic field should be completed with the cross-shock electric field. We do that (and the subsequent analysis) in the de Hoffman-Teller frame, assuming, in the spirit of *Hull et al.* [1998], that

$$\varphi(x) = \varphi_0 \frac{B(x) - B_u}{B_d - B_u}, \tag{2}$$

where B_u and B_d are the total upstream and downstream magnetic fields, respectively, and φ_0 is the overall (from upstream to downstream) cross-shock de Hoffman-Teller potential. This total potential drop is taken from the *Schwartz et al.* [1988] estimate $e\varphi_0 = 0.15(m_i V_u^2/2)$ for this particular shock (the potential estimates were kindly provided to us by S. Schwartz). The functional form (2) implies nearly adiabatic behavior of electrons and cannot be checked observationally unless one has high-resolution (faster than one distribution in 1 s) electron measurements, which is not realistic at the present stage. Nevertheless, in the absence of a better approximation and in view of the indications of the validity of (2), at least for those shocks where the resolution is sufficient (J. Scudder, private communication, 1998), we shall adopt this potential distribution as a working hypothesis. The normal incidence frame potential can be found using an integration of the noncoplanar magnetic field across the shock. Since it does not appear in our analysis below, we do not perform such integration here.

The electric field itself is found as $E_x = -d\varphi/dx$, where we must know how to convert the time measured by the spacecraft into a spatial coordinate. Direct estimates (the spatial separation divided by the time separation along with the density measurements) give the shock velocity as $V_{sh} = 0.08(c/\omega_{pi})/\mathrm{s}$. Given the substantial uncertainties in the shock normal determination as well as possible errors in the density measurements, this is an order of magnitude estimate rather than an exact result. In what follows we use a slightly smaller coefficient, $1\ \mathrm{s} \to 0.06(c/\omega_{pi})$, for the conversion of measured temporal scales to spatial ones, for the reasons described in section 3. Here we only mention that larger coefficients appear to be grossly inconsistent with even approximate shock stationarity. The so obtained electric field is shown in Figure 5, together with the total magnetic field.

The applied filtering procedure and chosen potential profile retain the substructure of the ramp, in contrast with the usual smoothing of it (compare with the model shock profile suggested by *Scudder et al.* [1986a]). For comparison we show different levels of filtering in Figure 6. The more smoothed profiles appear closer to the standard theoretical shock structure. However, numerical analysis of the ion motion (see section 3) shows that such smooth profiles cannot be maintained when quasi-stationary or slowly varying and that the small-scale structure has to be retained.

3. Ion Dynamics

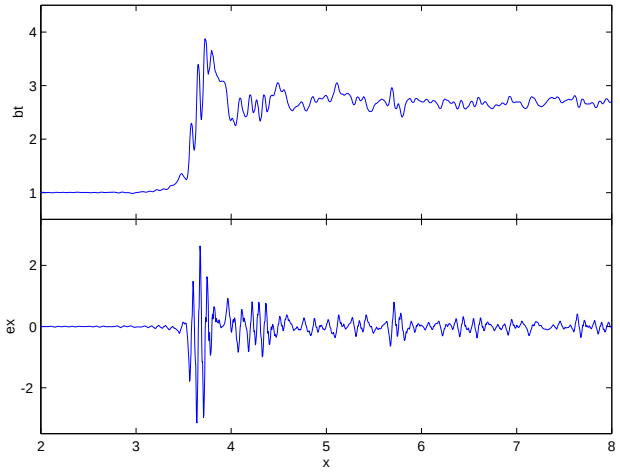

Figure 5. Total normalized magnetic field $|\mathbf{B}|/B_u$ and de Hoffman-Teller electric field E_x/E_{yu} (where $E_{yu} = V_u B_u \sin\theta$) in the shock front. The electric field is $\propto dB/dx$. Time is transformed into spatial coordinates using $1\,\mathrm{s} = 0.06(c/\omega_{pi})$. The coefficient of proportionality is found from observations and corrected after numerical analysis of ion motion (see section 3).

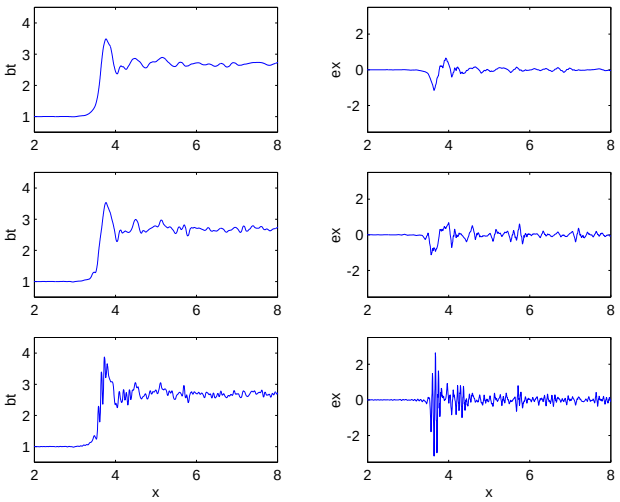

Figure 6. Magnetic field filtered using Daubechies 10 wavelet transform and removing four, three, and two finest levels, respectively, and the corresponding electric field. Numerical analysis of ion motion (bottom profile) shows that wider profiles (upper two profiles) result in stronger ion reflection and gyration, so that pressure balance cannot be maintained.

After the shock is prepared for numerical analysis of the particle motion, we trace ions assuming an upstream Maxwellian distribution with $\beta_i = 0.05$ (which corresponds to the thermal ion velocity $v_{Ti}/V_u = 0.048$; that is, the thermal spread of the incident ions is very low). Figure 7 shows trajectories of 100 ions in the shock front. The motion is in agreement with recent theoretical predictions [*Gedalin*, 1996a, 1997b] and extends the previous numerical analysis of *Zilbersher et al.* [1998]: the ions strongly gyrate behind the ramp, and the fraction of reflected ions is relatively low (the Mach number $M_A = 3.3$ is not especially high, albeit supercritical). There is some smoothing due to the small-scale structure and gyrophase mixing typical for an oblique geometry. Yet there is a clear bunching of ions at the gyration turning points downstream, which would result in strong local density enhancements. It should be noted that similar ion tracing in more smoothed profiles (Figure 6) or with larger shock velocities (a wider shock) results in much stronger ion reflection and gyration. The results were especially sensitive to the change of the scaling factor which converts temporal scales to spatial ones: ion reflection was rapidly enhanced when this factor was increased by even 10%. When the scale factor

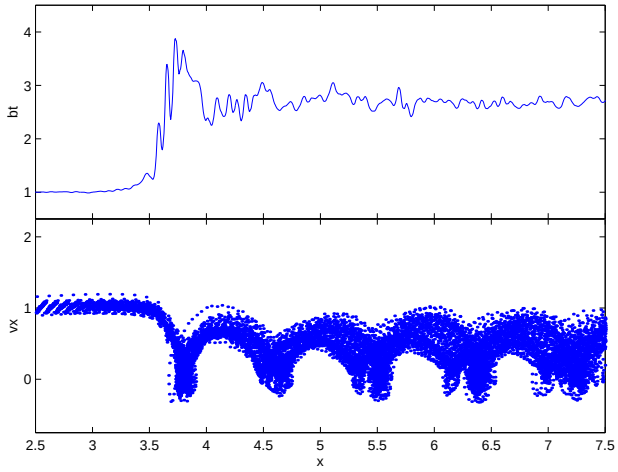

Figure 7. Trajectories of 100 ions: x measured in upstream convective ion gyroradii V_u/Ω_u ($\Omega_u = eB_u/m_i$) and components of $\mathbf{v}$ measured in upstream plasma velocities V_u. Downstream distribution of transmitted ions gyrates strongly with few reflected ions. Smoothing is due to the small-scale structure in the ramp and gyrophase mixing in oblique geometry. Downstream heating is due to the ion gyration and gyrophase mixing.

$0.08(c/\omega_{pi})/\mathrm{s}$ was used, the reflected ion fraction was found to be $\sim 40\%$ (compare with the $\approx 5\%$ reflection for the scale factor $0.06(c/\omega_{pi})/\mathrm{s}$), which is an enormous value for this moderate Mach number shock.

We proceed with the calculation of the ion hydrodynamical variables throughout the shock using the staying time method [*Veltri et al.*, 1990], where the relative contribution of a particle into the distribution in a thin layer is proportional to the time it spends in this layer. The numerically determined hydrodynamical characteristics are shown in Figures 8 (density and velocities) and 9 (pressure tensor). All hydrodynamical variables strongly fluctuate because of the weak smoothing. Although it could be expected that small-scale small-amplitude fluctuations may be smoothed out by improving statistics (1000 ions were traced), by the presence of low-amplitude waves in the real profile, and by averaging over wider layers (as it is in fact done by spacecraft devices), the large-amplitude fluctuations, as seen in density, are generic and due to insufficient smoothing in the regular fields: the ion distribution almost stops as a whole in certain positions. Slow variations of the shock profile would improve the situation by spreading these turning ions over a spatial scale determined by the distance to which the nonstationary feature moves in one ion gyroperiod. The gyration ions move by about one convective gyroradius along the shock front, so that if the shock front is inhomogeneous, the ions with rather different initial conditions would meet in the same point downstream, thus making the ion distribution substantially more diffuse.

The diagonal component of the ion pressure is one of the largest terms in the pressure balance equation (1). This pressure starts to build up in the foot ahead of the ramp, owing to the contribution of reflected ions (their contribution to the ion density is negligible), because of their velocities $\sim V_u$ there. Quick comparison shows that the pressure balance is satisfied only approximately (electron contribution is only a small part). Test runs with smoother shock profiles or wider shock scales have resulted in much larger $p_{i,xx} \approx n_u m_i V_u^2$ which is impossible in a quasi-stationary profile and which would result in fast shock breaking. We conclude that the shock has to be sufficiently narrow in order to not reflect too many ions. The small-scale structure effectively reduced the shock width working in this direction. This conclusion, unexpected at the first sight, is related to the fact that the magnetic field B_z, integrated across the ramp, affects positively on ion reflection [*Leroy et al.*, 1982; *Burgess et al.*, 1989; *Gedalin*, 1996a], thus reduction of $\int B_z dx$ would help to reduce the reflection. Presently, it is not clear why the whole shock ramp does not narrow to smaller scales but prefers to develop a small-scale substructure. It may be related to the ramp stability problems arising when the current $\propto dB_z/dx$ becomes too high.

The noncoplanar component of the ion pressure $p_{i,xy}$ is related to the noncoplanar magnetic field [*Gedalin*, 1996b]. Large $p_{i,xy}$ shows that the deviations from the simple expression by *Jones and Ellison* [1987, 1991] may be substantial.

4. Electron Dynamics

We proceed with the analysis of the electron dynamics. It should be understood that collisionless electron motion in the shock front is only a part of the story, since eventual shape of the electron distribution and final heating cannot be explained in the framework of the collisionless approach only and require additional mechanisms. In particular, the substantial gap [*Hull et al.*, 1998; *Gedalin et al.*, 1997; *Gedalin and Griv*, 1999a] in the electron distribution, resulting from the collisionless acceleration by the cross-shock electric field (see below) has to be filled to agree with observations. This filling may be

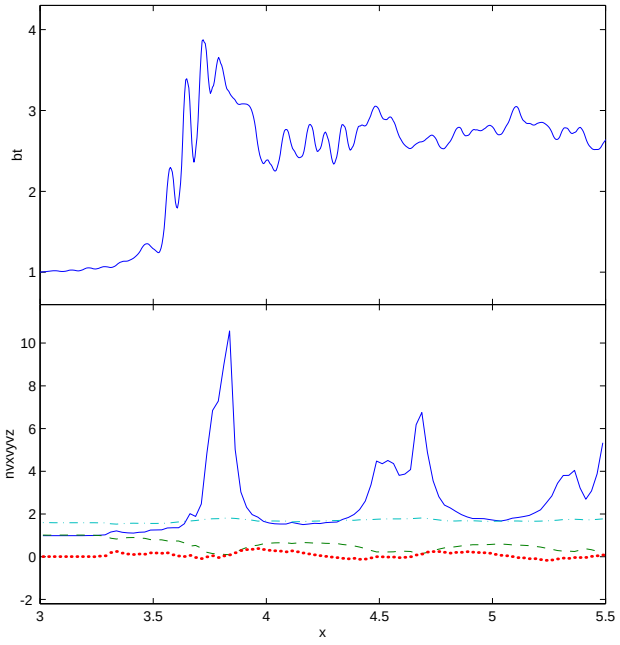

Figure 8. Hydrodynamical characteristics of the downstream ion distribution: density n/n_u (solid line) strongly increases at the overshoot, V_x/V_u (dashed line) decreases at the overshoot almost down to zero, V_y/V_u (dotted line) weakly oscillates around zero, and V_z/V_u (dash-dotted line) almost does not change. Large "overshoots" of the density are due to insufficient smoothing (gyration of the downstream ion distribution as a whole, because of which the ion "beam" almost stops each $\approx 2(V_u/\Omega_d)$.

achieved either as a result of some preexisting electron population [*Feldman et al.*, 1982; *Feldman*, 1985] or as a result of instabilities in the shock front [*Veltri et al.*, 1990, 1992 ; *Veltri and Zimbardo*, 1993a, b; *Gedalin*, 1999]. Therefore analysis of collisionless electron motion does not provide complete information about electron temperature and density after crossing the ramp. It rather describes the behavior of the high-energy tail of the electron distribution function, which is expected to not be changed much during subsequent instabilities and quasi-linear/nonlinear relaxation [*Gedalin*, 1999; *Gedalin and Griv*, 1999b].

It should also be mentioned that electron dynamics are sensitive to the small-scale inhomogeneities of the electric field [see, e.g., *Balikhin et al.*, 1998], so that detailed knowledge of the electric field structure (probably including nonstationary features too) is, in principle, necessary for the comprehensive analysis of electron distributions in the shock front. Electric field measurements of this quality are not available to us at this stage, so in the absence of a better choice, we have to use the model electric field, following the assumptions by *Scudder et al.* [1986c]; *Schwartz et al.* [1988]; *Scudder* [1995], and *Hull et al.* [1998]. The results below are therefore obtained within a certain model (although widely accepted) and may be incorrect if the model is significantly wrong. Yet the analysis provides sufficiently important semi quantitative information about the electron behavior in the cross-shock fields to warrant performing it even if the fine-scale structure of the shock is not quite known.

For the numerical analysis we assume that the upstream electron distribution is Maxwellian with $\beta_e = 0.19$. This corresponds to $v_{Te}/V_u = 5.66$ and $v_{Te}\cos\theta/V_u = 2.83$; that is, upstream electrons are subsonic in the de Hoffman-Teller frame. This value of β_e is based on the assumed value of electron upstream temperature $T_e = 141,000$ K, in the absence of direct electron temperature measurements, and differs from *Schwartz et al.* [1988] where $\beta_e = 0.05$. Figure 10 shows the trajectory of a single electron with the upstream velocity $(V_u, 0, V_u\tan\theta)$ in the de Hoffman-Teller frame. This velocity is along the upstream magnetic field, and initially the perpendicular component of the velocity is absent. In the completely adiabatic case this electron would cross the shock moving along the magnetic field. In reality it acquires some gyration energy, but the fraction of the cross-shock potential transformed into this energy is small.

Figure 11 shows the trajectories of 50 electrons crossing the shock. The electrons are initially Maxwellian. Those electrons having upstream $v_{\|} < 0$ leak from the downstream region and are also present in the distribution. Part of the electrons seen upstream (corresponding to the downstream $v_z < 0$) are these leaking electrons. Another part of the upstream electron distribution are reflected electrons. The downstream distribution is diffuse and heated in the direction perpendicular to the magnetic field (the electron distribution is substantially wider in x and y directions). It is difficult to speak about

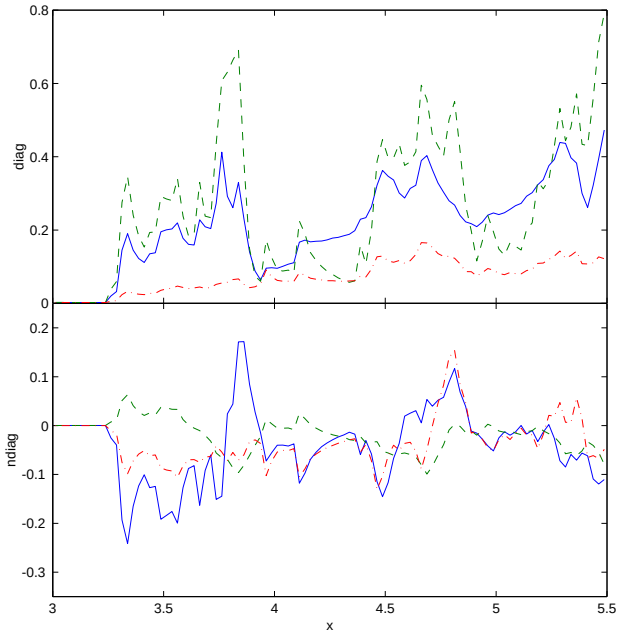

Figure 9. Hydrodynamical characteristics of the downstream ion distribution: diagonal components of pressure (normalized on $n_u m_i V_u^2$) p_{xx} (solid line), p_{yy} (dashed line), p_{zz} (dash-dotted lline), and off-diagonal components p_{xy} (solid line), p_{xz} (dashed line), p_{yz} (dash-dotted line). Pressure balance across the shock front requires $nmV_x^2 + p_{xx} + B^2/2\mu_0 = \text{const}$, which is satisfied only approximately in this case. The non-diagonal pressure p_{xy} is related to the noncoplanar component of the magnetic field.

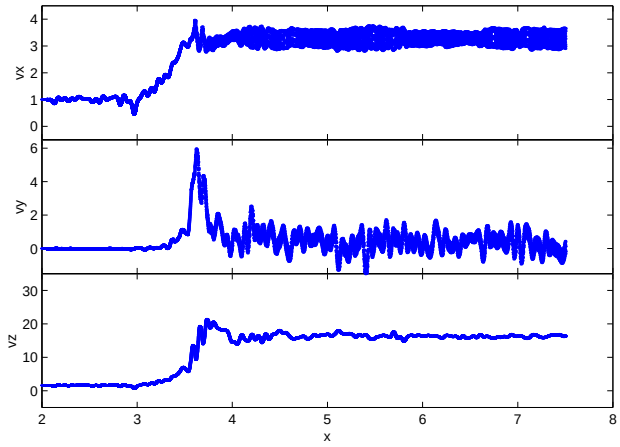

Figure 10. Trajectory of a single electron starting with the velocity $(V_u, 0, V_u \tan\theta)$ in the de Hoffman-Teller frame. The motion is almost adiabatic: downstream gyration velocity is $\sim V_u$ but substantially less than the upstream electron thermal velocity. Only a small fraction of the cross-shock potential is transformed into the electron gyration energy.

parallel heating before the gap in the distribution (between the transmitted and back-streaming electrons) is filled and the distribution becomes smooth enough. This widening of the electron distribution (heating) occurs already at the ramp (compare with the magnetic field profile and the ion behavior in Figure 7).

The projection of the phase space filled by electrons on the $v_x - v_y$ plane is shown in Figure 12. Transmitted, reflected, and back-streaming electrons are separated for clarity. It should be noted that the shown distribution is not properly weighted with the staying time taken into account, so that it is not what may be measured. In particular, it cannot be used directly for density estimates. It is rather the direct numerical Liouville mapping, where we numerically determine, for the given Maxwellian of 100 upstream electrons, the electrons' velocities at some downstream position. Figure 12c panel shows the

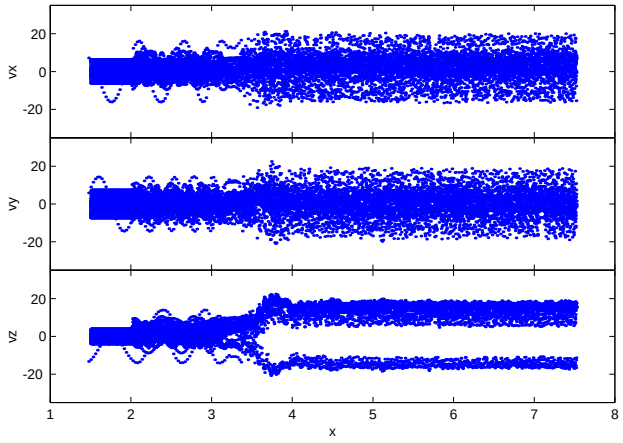

Figure 11. Trajectories of 50 electrons. The downstream distribution is diffuse and heated. Some of the downstream electrons are back-streaming electrons. Strong heating occurs in the ramp. Part of the electrons seen upstream are reflected electrons, and another part are back-streaming electrons.

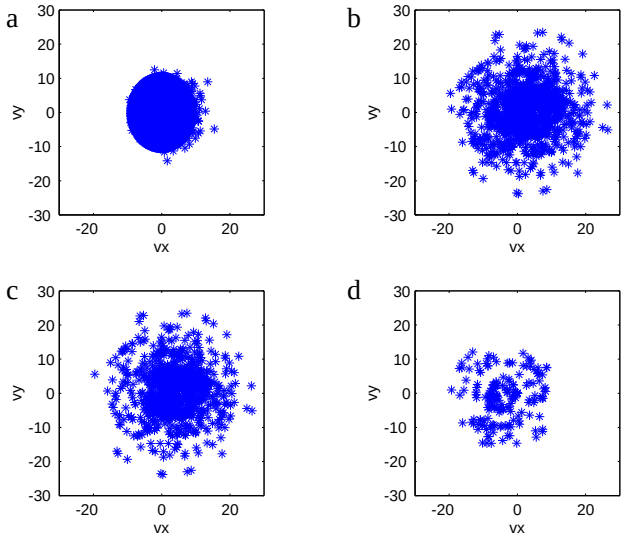

Figure 12. Unweighted distribution of electrons in $v_x - v_y$ plane: (a) upstream, including initial Maxwellian, back-streaming, and reflected electrons; (b) downstream, including transmitted and back-streaming electrons; (c) downstream transmitted electrons; and (d) downstream back-streaming electrons.

transmitted electrons. The plane $v_x - v_y$ is almost perpendicular to the downstream magnetic field, so that the Figure 12c shows qualitatively the perpendicular energy increase of the transmitted electrons. At the first sight the downstream distribution is twice as wide as the initial distribution, which corresponds to the perpendicular temperature $T_{d,\perp} \approx 4T_{u,\perp}$ and slightly exceeds the adiabatic value $B_d/B_u \approx 2.7$. However, quantitative determination of the temperature requires knowledge of the true distribution (proper weighted density in the phase space) and can give results that are different from the above oversimplified estimate. For the reasons explained above we do not provide temperature estimates here. There is a substantial number of backstreaming electrons (Figure 12d) which is because of the large value of $\beta_e = 0.19$ (and therefore v_{Te}/V_u) used in the present numerical analysis.

The evolution of the unweighted electron distribution
across the shock front is shown in Figure 13. These "distributions" are found by accumulating electrons caught in a number of layers of width $0.05(V_u/\Omega_u) \approx 0.17(c/\omega_{pi})$. This layer width approximately corresponds to the 3 s resolution of ISEE particle measurements. Acceleration along the magnetic field due to the cross-shock potential (with the pronounced gap in the electron distribution) and sudden perpendicular heating at the ramp are clearly seen.

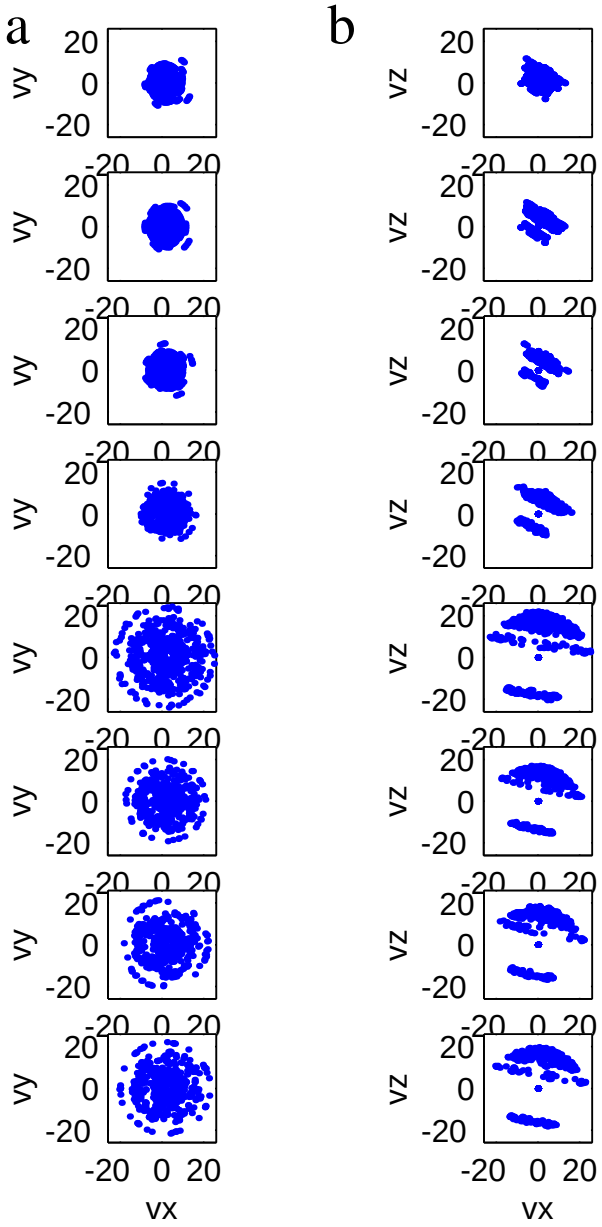

Figure 13. Evolution of electron distribution across the shock in the (a) $v_x - v_y$ plane and (b) $v_x - v_z$ plane. The distributions are accumulated in the following intervals (from top to bottom): $2 < x < 2.05$, $3 < x < 3.05$, $3.25 < x < 3.2$, $3.5 < x < 3.55$, $3.75 < x < 3.8$, $4 < x < 4.05$, $4.25 < x < 4.3$, and $4.5 < x < 4.55$ (x measured in V_u/Ω_u).

5. Conclusions

We have performed a numerical analysis of the charged particle (ions and electrons) motion in the front of an observed supercritical, quasi-perpendicular shock in order to test whether the observed magnetic field is consistent with the one-dimensional stationary model. In this model the ion reflection and gyration, which result in efficient heating, are determined by the ion dynamics in the quasi-static electric and magnetic fields of the shock front. To this purpose, we had to remove nonstationary features. The filtering procedure is not free of some arbitrariness, and the result of the analysis may depend on the particular scheme and level of filtering. The chosen wavelet filtering retains the sharp gradients while removing quasiperiodic oscillations and is expected to interfere with the physically meaningful scales. The usual level of filtering assumes that all large-amplitude, small-scale features should be smoothed out. We have found that such a smooth profile (with the same cross-shock potential and shock width) would result in ion reflection that is too strong and a pressure balance that cannot be maintained, so that the shock profile would be strongly nonstationary. Since two-spacecraft measurements do not provide evidence of such nonstationarity, we conclude that the small-scale features are an important part of the shock

structure and necessary for shock stability. When scaling the shock front, we have also found that if the shock is wider, the ion reflection and gyration are too strong to be consistent with the stable quasi-stationary shock profile. In other words, the narrowing of the ramp and its breaking into several subramps reduce the ion reflection down to the level where pressure balance and therefore quasi-stationary shock stability can be maintained. We speculate that the substructure is formed when especially strong narrowing of the ramp is necessary, although it is not clear what determines the particular shock behavior.

In view of the above analysis we suggest the following qualitative picture of the shock formation. Consider the initial piston as a large-amplitude magnetosonic wave. It is known to nonlinearly steepen in the nondispersive MHD range when the typical scale is $\gtrsim c/\omega_{pi}$ [see, e.g., *Kennel et al.*, 1985]. For shorter scales (wavelengths) the magnetosonic waves become dispersive. However, it was shown [*Krasnosel'skikh*, 1985; *Gedalin*, 1988] that this dispersion cannot prevent further steepening (which stops only when the width (wavelength) becomes of the order of the whistler length $c\cos\theta/M_A\omega_{pi}$ [*Gedalin*, 1998]) when steepening
changes to the magnetic field rotation. This conclusion is valid for the smooth behavior of the ion pressure across the shock front. Since the above analysis shows that the ion pressure does not change drastically across the ramp, the above should qualitatively describe the ramp steepening, and the ramp width can be expected to be of the order of the whistler length. At this scale the ion reflection is already substantial, and the eventual ramp width should be determined by the adjustment of the reflected ion distribution so that the pressure balance is approximately satisfied.

Let us now assume that the ramp for some reason becomes less steep. As is shown above, the ion reflection enhances with the clear cut pressure maximum just behind the overshoot. This extra ion pressure pushes the overshoot toward upstream, thus causing the ramp steepening. If, on the other hand, the ramp becomes steeper, the ion pressure just behind the overshoot decreases, so that the overshoot is pulled toward downstream, causing ramp desteepening. This process may lead to a quasi-stationary (or slowly moving) ramp or to an oscillatory shock front. This qualitative explanation of the ramp formation should not be considered as a substitute for a more sophisticated theory but rather as a suggestion for further study which is beyond the scope of the present paper. In particular, the mechanism of the ramp breakdown into several narrower subramps is unclear (one possibility is the overturning proposed by *Krasnosel'skikh* [1985]).

We have also found that despite the fact that the energetics of the ion dynamics could be satisfactorily explained by their motion in the stationary one-dimensional shock front, the resulting ion distribution fluctuations are far too strong in comparison with observations and, most probably, would imply shock profile instability. We conclude that the shock has to be inhomogeneous along the shock profile (three-dimensional shock structure or rippling) at the reflected ion spatial scale $\sim V_u/\Omega_u$ in order to smooth out the ion distributions. The observed weak nonstationarity of the shock front also contributes to this smoothing.

We have found that in this particular shock, despite the large cross-shock de Hoffman-Teller potential, electrons behave adiabatically. This conclusion is less reliable, however, since electrons are very sensitive not only to the width of the small-scale features but also to the fine details of the electric field distribution, which are not known and which are affected by the filtering procedure. The electron distribution also depends very much on the upstream β_e and on the unknown mechanism of the gap filling. These uncertainties do not allow us to directly check the pressure balance condition, which requires knowledge of the electron pressure. However, estimates show that the electron contribution is still substantially less than the found mismatch (deviations from the pressure balance constancy across the shock).

To conclude, observations show that the shock is approximately (but only to a certain degree) quasi-stationary and weakly inhomogeneous in the direction along the shock normal, which allows us to apply the stationary one-dimensional model as a first-order approximation. Narrow shock width and small-scale structure are necessary to reduce ion reflection down to an appropriate level. Further ion distribution smoothing is required to ensure the stability of the shock profile, and this smoothing has to be achieved through three dimensionality of the shock front and weak nonstationarity.

Acknowledgments. We are grateful to S. Schwartz for kindly providing his estimates of the cross-shock potential. Wavelet transform has been done using Matlab with the Wavelab package. The research was supported in part by Israel Science Foundation under grant 261/96-1.

Hiroshi Matsumoto thanks F. Jones and another referee for their assistance in evaluating this paper.

References

Balikhin, M., M. Gedalin, and A. Petrukovich, New mechanism for electron heating in shocks, *Phys. Rev. Lett., 70,* 1259, 1993.

Balikhin, M., V.V. Krasnosel'skikh, L.J.C. Woolliscroft, and M. Gedalin, A study of the dispersion of the electron distribution in the presence of E and B gradients: application to electron heating at quasi-perpendicular shocks, *J. Geophys. Res., 103,* 2029, 1998.

Burgess, D., W.P. Wilkinson, and S.J. Schwartz, Ion distribution and thermalization at perpendicular and quasi-perpendicular supercritical collisionless shocks, *J. Geophys. Res., , 94,* 8783, 1989.

Feldman, W.C., Electron velocity distributions near collisionless shocks, in *Collisionless Shocks in the Heliosphere: Reviews of Current Research, Geophys. Monogr. Ser.,* vol. 35, edited by R.G. Stone and B.T. Tsurutani, p. 195, AGU, Washington, D. C., 1985.

Feldman, W.C., S.J. Bame, S.P. Gary, J.T. Gosling, D. McComas, M.F. Thomsen, G. Paschmann, N. Sckopke, M.M. Hoppe, and C.T. Russell, Electron heating within the Earth's bow shock, *Phys. Rev. Lett., 49,* 199, 1982.

Gedalin, M.E., Nonlinear magnetosonic waves in a hot plasma, *Sov. J. Plasma Phys., Engl.Transl., 14,* 346, 1988.

Gedalin, M., Ion reflection at the shock front revisited, *J. Geophys. Res., 101,* 4871, 1996a.

Gedalin, M., Noncoplanar magnetic field in the collisionless shock front, *J. Geophys. Res., 101,* 11,153, 1996b.

Gedalin ,M., Ion distributions at the quasiperpendicular collisionless shock front, *Surv. Geophys., 18,* 541, 1997a.

Gedalin, M., Ion heating in oblique low-Mach number shocks, *Geophys. Res. Lett., 24,* 2511, 1997b.
Gedalin, M., Low-frequency nonlinear stationary waves and fast shocks: Hydrodynamical description, *Phys. Plasmas, 5,* 127, 1998.
Gedalin, M., Two-stream instability of electrons in the shock front, *Geophys. Res. Lett., 26,* 1239, 1999.
Gedalin, M., and E. Griv, Role of overshoots in the formation of the downstream distribution of adiabatic electrons, *J. Geophys. Res., 104,* 14,821, 1999a.
Gedalin, M., and E. Griv, Collisionless electrons in a thin high Mach number shock: Dependence on angle and β, *Ann. Geophys.,* in press, 1999b.
Gedalin, M., K. Gedalin, M. Balikhin, and V.V.Krasnoselskikh, Demagnetization of electrons in the electromagnetic field structure, typical for quasi-perpendicular collisionless shock front, *J. Geophys. Res., 100,* 9481, 1995.
Gedalin, M., U. Griv, and M.A. Balikhin, Width dependent collisionless electron dynamics in the static fields of the shock ramp, 2, Phase space portrait, *Nonlinear Proc. Geophys., 4,* 173, 1997.
Gedalin, M., J. Newbury, and C.T. Russell, Shock profile analysis using wavelet transform, *J. Geophys. Res., 103,* 6503, 1998.
Goodrich, C.C., and J.D. Scudder, The adiabatic energy change of plasma electrons and the frame dependence of the cross shock potential at collisionless magnetosonic shock waves, *J. Geophys. Res., 89,* 6654, 1984.
Gosling, J.T., and M.F. Thomsen, Specularly reflected ions, shock foot thicknesses, and shock velocity determinations in space, *J. Geophys. Res., 90,* 9893, 1985.
Hull, A.J., J.D. Scudder, L.A. Frank, W.R. Paterson, and M.G. Kivelson, Electron heating and phase space signatures at strong and weak quasi-perpendicular shocks, *J. Geophys. Res., 103,* 2041, 1998.
Jokipii, J.R., J. Kota, and J. Giacalone, Perpendicular transport in 1- and 2-dimensional shock simulations, *Geophys. Res. Lett., 20,* 1759, 1993.
Jones, F.C., and D.C. Ellison, Noncoplanar magnetic fields, shock potentials, and ion deflection, *J. Geophys. Res., 92,* 11,205, 1987.
Jones, F.C., and D.C. Ellison, The plasma physics of shock acceleration, *Space Sci. Rev., 58,* 259, 1991.
Jones, F.C., J.R. Jokipii, and M.G. Baring, Charged-particle motion in electromagnetic fields having at least one ignorable spatial coordinate, *Astrophys. J., 509,* 238, 1998.
Kennel, C.F., J.P. Edmiston, and T. Hada, A quarter century of collisionless shock research, in *Collisionless Shocks in the Heliosphere: A Tutorial Review, Geophys. Monogr. Ser.,* vol. 34, edited by R.G. Stone and B.T. Tsurutani, p. 1, AGU, Washington, D. C., 1985.
Krasnosel'skikh, V., Nonlinear motions of a plasma across a magnetic field, *Sov. Phys. JETP, Engl. Transl., 62,* 282, 1985.
Leroy, M.M., D. Winske, C.C. Goodrich, C.S. Wu, and K. Papadopoulos, The structure of perpendicular bow shocks, *J. Geophys. Res., 87,* 5081, 1982.
Newbury, J.A., and C.T. Russell, Observations of a very thin collisionless shock, *Geophys. Res. Lett., 23*, 781, 1996.
Newbury, J.A., C.T. Russell, and M. Gedalin, The ramp widths of high-Mach-number, quasi-perpendicular collisionless shocks, *J. Geophys. Res., 103,* 29,581, 1998.
Schwartz, S.J., M.F. Thomsen, S.J. Bame, and J. Stansbury, Electron heating and the potential jump across fast mode shocks, *J. Geophys. Res., 93,* 12,923, 1988.
Sckopke, N., G. Paschmann, S.J. Bame, J.T. Gosling, and C.T. Russell, Evolution of ion distributions across the nearly perpendicular bow shock: Specularly and nonspecularly reflected-gyrating ions, *J. Geophys. Res., 88,* 6121, 1983.
Sckopke, N., G. Paschmann, A.L. Brinca, C.W. Carlson, and H. Lühr, Ion thermalization in quasi-perpendicular shocks involving reflected ions, *J. Geophys. Res., 95,* 6337, 1990.
Scudder, J.D., A review of the physics of electron heating at collisionless shocks, *Adv. Space Res., 15*(8/9), 181, 1995.
Scudder, J.D., A. Mangeney, C. Lacombe, C.C. Harvey, T.L. Aggson, R.R. Anderson, J.T. Gosling, G. Paschmann, and C.T. Russell, The resolved layer of a collisionless, high β, supercritical, quasi-perpendicular shock wave, 1, Rankine-Hugoniot geometry, currents, and stationarity, *J. Geophys. Res., 91,* 11,019, 1986a.
Scudder, J.D., A. Mangeney, C. Lacombe, C.C. Harvey, and T.L. Aggson, The resolved layer of a collisionless, high β, supercritical, quasi-perpendicular shock wave, 2, Dissipative fluid electrodynamics and stationarity, *J. Geophys. Res., 91,* 11,053, 1986b.
Scudder, J.D., A. Mangeney, C. Lacombe, C.C. Harvey, C.S. Wu, and R.R. Anderson, The resolved layer of a collisionless, high β, supercritical, quasi-perpendicular shock wave, 3, Vlasov electrodynamics, *J. Geophys. Res., 91,* 11,075, 1986c.
Thomsen, M.F., M.M. Mellott, J.A. Stansbury, S.J. Bame, J.T. Gosling, and C.T. Russell, Strong electron heating at the Earth's bow shock, *J. Geophys. Res., 92,* 10,119, 1987.
Veltri, P., and G. Zimbardo, Electron - whistler interaction at the Earth's bow shock, 1, Whistler instability, *J. Geophys. Res., 98,* 13,325, 1993a.
Veltri, P., and G. Zimbardo, Electron - whistler interaction at the Earth's bow shock, 2, Electron pitch angle diffusion, *J. Geophys. Res., 98,* 13,335, 1993b.
Veltri, P., A. Mangeney, and J.D. Scudder, Electron heating in quasi-perpendicular shocks: A Monte-Carlo simulation, *J. Geophys. Res., 95,* 14,939, 1990.
Veltri, P., A. Mangeney, and J.D. Scudder, Reversible electron heating vs. wave-particle interactions in quasi-perpendicular shocks, *Nuovo Cimento Soc. Ital. Fis. C, 15,* 607, 1992.
Woods, L.C., On double structured, perpendicular, magneto-plasma shock waves, *J. Plasma Phys., 13,* 281, 1971.
Zilbersher, D., M. Gedalin, J.A. Newbury, and C.T. Russell, Direct numerical testing of stationary shock model with low Mach number shock observations, *J. Geophys. Res., 103,* 26,775, 1998.